NASA CONTRACTOR
REPORT

NASA CR-61106

NASA CR-61106



# LUNAR DUST/DEBRIS HAZARDS ASSOCIATED WITH THE MANNED FLYING SYSTEM

Prepared under Contract No. NAS 8-20082 by

R. L. Stark, F. B. Tatom, L. M. Bhalla,
and Dr. H. W. HSU

NORTHROP SPACE LABORATORIES
Huntsville Department
Huntsville, Alabama



For

NASA-GEORGE C. MARSHALL SPACE FLIGHT CENTER
Huntsville, Alabama

October 1965

October 1965 NASA CR-61106

# LUNAR DUST/DEBRIS HAZARDS ASSOCIATED WITH THE MANNED FLYING SYSTEM

By

R. L. Stark, F. B. Tatom, L. M. Bhalla,
and Dr. H. W. Hsu



Prepared under Contract No. NAS 8-20082 by

NORTHROP SPACE LABORATORIES
Huntsville Department
Huntsville, Alabama

NASA-GEORGE C. MARSHALL SPACE FLIGHT CENTER

## ABSTRACT

10703

The results are presented of a preliminary investigation to determine the nature of potential hazards associated with the impingement of the exhaust gases of the Manned Flying System (MFS) on a dust - and/or debris-covered lunar surface. An engineering model is established based on the results of preceding investigations. The behavior of individual particles of dust, set in motion by jet impingement, is predicted. The results indicate that there is a possibility of dust/debris directly striking the MFS only at very low altitudes (less than six feet) with impingement craters of small radii (less than 4.5 feet). The distance out to which particles are thrown is considerable, however, ranging as high as 1200 miles, and the possibility does exist that particles may strike personnel or equipment on the lunar surface in the vicinity of the landing site of the MFS. The possibility also exists that, during the descent or ascent of the MFS in the proximity of sheer, vertical surfaces, projected particles may ricochet off such surfaces and then strike the MFS. Author

## FOREWORD

The investigation described in this report was requested by Mr. Lynn L. Bradford of the Systems Concepts Planning Office, Aero-Astrodynamics Laboratory, George C. Marshall Space Flight Center. The study was carried out by Mr. F. B. Tatom, Mr. Robert L. Stark, Dr. H. W. Hsu, and Mr. L. M. Bhalla of the Huntsville Department of Northrop Space Laboratories, under Contract No. NAS8-20082, Appendix F-1, Schedule Order No. 4, Technical Directive No. 4. Work commenced on 20 July and ended on 4 October 1965 with a total of 6 man-weeks expended.

TABLE OF CONTENTS

## DEFINITION OF SYMBOLS

### A. English Letters

| Symbol | Definition | Units |
|---|---|---|
| $A_{ef}$ | effective particle area | $ft^2$ |
| $C_e$ | entrainment coefficient | $(ft^3/lb_m)^{\frac{1}{2}}$ |
| $c_p$ | specific heat at constant pressure | $\frac{lb_f\ ft}{lb_m\ ^\circ R}$ |
| e | eccentricity defined by Eq. (2-18) | - |
| $F_f$ | static friction force | $lb_f$ |
| $F_s$ | surface shearing force | $lb_f$ |
| $f_d$ | static friction factor of dust | - |
| $g_m$ | acceleration due to lunar gravity | $ft/sec^2$ |
| h | height of MFS above lunar surface | ft |
| k | dimensionless parameter ( $=\gamma(\gamma-1)M_n^2$) | - |
| $M_n$ | Mach number at nozzle exit | - |
| P | pressure of gas | $lb_f/in^2$ |
| $P_r$ | normal shock recovery pressure | $lb_f/in^2$ |
| $P_s$ | stagnation pressure | $lb_f/in^2$ |
| R | distance measured from nozzle exit | ft |
| $R_m$ | lunar radius | ft |
| $R_o$ | specific gas constant | $\frac{lb_f\ ft}{lb_m\ ^\circ R}$ |
| $r_c$ | crater radius | ft |
| $r_n$ | exit radius of nozzle | ft |
| S | range of dust/debris particles | ft |
| T | temperature | $^\circ R$ |
| $T_s$ | stagnation temperature | $^\circ R$ |
| t | time | sec |

| Symbol | Definition | Units |
|---|---|---|
| $U$ | velocity of gas | ft/sec |
| $U_c$ | gas velocity at crater edge | ft/sec |
| $V_d$ | velocity of dust particle | ft/sec |
| $V_x$ | velocity in x-direction | ft/sec |
| $V_y$ | velocity in y-direction | ft/sec |
| $v_d$ | volume of individual particle | $ft^3$ |
| $x$ | distance along lunar surface | ft |
| $y$ | distance above lunar surface | ft |

## B. Greek Letters

| | | |
|---|---|---|
| $\beta$ | surface angle measured from horizontal | rad |
| $\gamma$ | ratio of specific heats | - |
| $\theta$ | angle measured from the vertical centerline of jet | rad |
| $\theta_c$ | the value of $\theta$ corresponding to $r_c$ | rad |
| $\mu$ | viscosity of gas | $\frac{lb_m}{ft\ sec}$ |
| $\mu_m$ | lunar gravitational constant | $ft^3/sec^2$ |
| $\rho$ | density of gas | $lb_m/ft^3$ |
| $\rho_c$ | gas density at crater edge | $lb_m/ft^3$ |
| $\rho_d$ | density of dust particles | $lb_m/ft^3$ |
| $\rho_n$ | gas density at nozzle exit | $lb_m/ft^3$ |
| $\rho_o$ | gas chamber density | $lb_m/ft^3$ |
| $\rho_r$ | normal shock recovery density of gas | $lb_m/ft^3$ |
| $\rho_s$ | stagnation density of gas | $lb_m/ft^3$ |
| $\tau_s$ | shear stress | $lb_f/ft^2$ |

## SUMMARY

A preliminary study has been conducted to determine the hazards associated with the impingement of the exhaust gases of the Manned Flying System (MFS) on a dust-/debris-covered lunar surface. The study consisted of a survey of previous pertinent investigations, and the development and application of a simplified engineering model to predict the impingement and entrainment phenomena.

Three potential hazards are discussed: (1) reduced visibility during ascent or descent, (2) the striking of the MFS by lunar dust or debris, and (3) the striking of personnel and equipment on the lunar surface by lunar dust/debris. Major emphasis was placed on the latter two hazards. The results obtained from applying the engineering model indicate that the possibility of particles directly striking the MFS only occurs at very low altitudes with small impingement crater radii. There is, however, also the possibility of particles ricocheting off of sheer vertical portions of the lunar terrain and then striking the MFS from above or from the side. Finally, there exists a region, extending out as far as 1200 miles from the impingement site, in which lunar dust or debris may rain down on personnel and equipment on the lunar surface.

# 1.0 INTRODUCTION

There is a strong possibility that the lunar surface is covered with a layer of dust and/or debris ranging in depth from one to twenty feet. The exhaust gases from the Manned Flying System, during descent to a previously undisturbed portion of the lunar surface, would impinge upon such a dust layer. The effects of this impingement could conceivably represent a hazard to the astronauts aboard the MFS. Thus it is important to determine the exact nature and magnitude of the impingement of the rocket exhaust gases on a dust-covered surface, and also the subsequent behavior of dust or debris set in motion by such impingement.

A number of investigations (refs. 1 through 8) have been conducted which were concerned with the problem of jet impingement on a dust-covered surface in a vacuum. Most of these (refs. 1, 2, 3, 6, 7, and 8) were primarily experimental in nature. The results obtained generally indicate that a symmetrical crater will be formed by the jet impingement. Dust and debris will be projected outward from this crater forming a cloud composed of particles of various sizes. Because of the absence of an atmosphere, the individual particles will rapidly settle out and the cloud will thus dissipate. Visibility in the vicinity of the point of impingement will be affected, especially during the last few seconds of descent of the vehicle.

Unfortunately, due to the number of parameters involved in the phenomenon under consideration, experimental studies have not provided a means of predicting the behavior of individual bits of dust or debris.

Scaling of results have proven to be relatively unfruitful because of the complex nature of the impingement action. To remedy this situation several analytical investigations (refs. 4 and 5) have been carried out. As is the case in most engineering research, each of these studies was based on a series of simplifying assumptions. These assumptions were generally necessary in order to keep the problem tractable under the state-of-the-art at the time of the investigations. The results obtained were in the form of rather complicated equations for predicting various important parameters relating to the formation of the impingement crater and the motion of dust and debris. A certain amount of correlation between theoretical predictions and experimental data was attempted but it is difficult to assess the success achieved in such correlation.

There exists a definite need for a careful evaluation of all available literature on this subject, and for the development of an analytical model which contains a minimum of restricting assumptions and which is generally applicable without the need for scaling parameters or empirical constants.

This report presents the results of a preliminary study by the Huntsville Department of Northrop Space Laboratories concerning the effects of the exhaust jet of the Manned Flying System impinging on a dust-covered lunar surface. Because of time and manpower limitations, no attempt was made to develop a general theory. Instead, all available relevant literature was reviewed and a simple engineering model was established. By means of this model the approximate behavior of dust and debris following impingement was determined.

## 2.0 TECHNICAL DEVELOPMENT

### 2.1 Engineering Model

The engineering model chosen to describe the jet exhaust flow field, the erosion, and the subsequent transport of surface particles, is shown in Fig. 2-1.

Since the flow is hypersonic, it is undisturbed by the presence of the surface beneath the vehicle until it impinges on the surface, where a shock wave, approximately parallel to the surface, is formed.

On passing through the shock, the gas is diverted to flow primarily in a radial direction over the surface. A region of subsonic flow exists between the strong shock and the surface near the stagnation point. As the radius, r, increases, the flow behind the shock again becomes supersonic.

The flow over the surface produces a surface shearing force which is the primary force tending to set the dust particles in motion. The initial resistance to motion is the static friction force of the particles. Dust movement will commence when the surface shearing force exceeds the static force. As erosion takes place, the change in the surface profile alters the gas flow field and the imposed shear distribution This interaction is such as to create an expanding region of erosion beneath the vehicle.

The entrained particles will be directed upward by impact with the edge of this eroded region. The actual path of these particles will

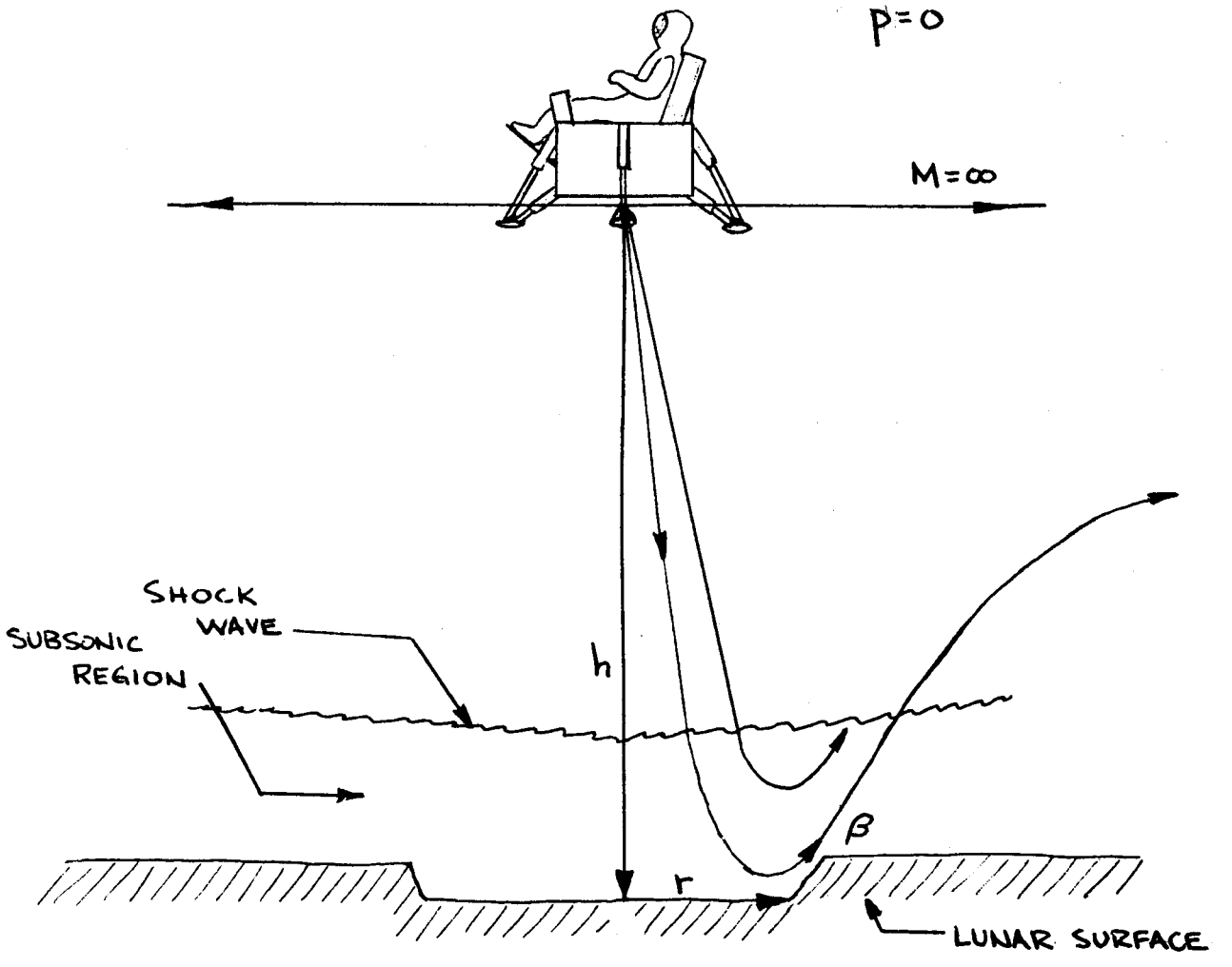


FIGURE 2-1. ENGINEERING MODEL FOR JET IMPINGEMENT WITH DUST-COVERED SURFACE

depend upon the distance the edge of the eroded region is from the vehicle and upon the mechanics of the particle collision with this edge.

A theoretical study of the described phenomena was attempted in ref. 4 as already noted. The result of that study was a series of complicated relationships which depend upon such dust properties as particle size and density, the dust cohesive strength, and the roughness of the lunar surface. Information on these lunar dust properties is obviously unavailable at this time. For this reason, in this study, the simplified engineering model was used as a basis for a parametric study to better establish the interelation between the important variables. The problem was treated in two parts: first, the expansion of a jet into a vacuum and the flow that exists between the strong shock and the flat surface; and second, the behavior of the particles due to the jet-surface interaction.

## 2.2 Exhaust Jet Impingement

### 2.2.1 Expansion of a Jet in a Vacuum

The expansion of the jet into the zero ambient pressure (vacuum) is unaffected upstream of the shock wave by the existence of the surface. The calculation of a jet expanding into a vacuum was accomplished in ref. 9 by using the method of characteristics for the isentropic and inviscid flow of a perfect gas. It was shown that in the far field the flow pattern approaches source point flow.

The essential character of the flow field is described quantitatively in ref. 4 by assuming a density profile which varies as $(\cos\theta)^k$ where $\theta$

is the angle measured from the vertical center line of the jet (Figure 2-2). The resulting expression for the density, $\rho$, on a spherical cap at a distance, R, from the nozzle exit is written

$$\frac{\rho}{\rho_n} = \frac{k}{2} \left(\frac{R}{r_n}\right)^{-2} (\cos\theta)^k \text{ (upstream of shock)} \qquad (2\text{-}1)$$

where

$\rho_n$ = gas density at nozzle exit

$r_n$ = exit radius of nozzle

$k = \gamma(\gamma - 1) M_n^2$

$\gamma$ = ratio of specific heats

$M_n$ = Mach number at nozzle exit.

2.2.2 Flow Region Downstream of Shock

The surface pressure, P, is found by considering the flux of momentum toward the surface (reference 4) and is given by

$$P = \frac{k+2}{2} P_r \left(\frac{h}{r_n}\right)^{-2} (\cos\theta)^{k+4} \qquad (2\text{-}2)$$

where

$P_r$ = normal shock recovery pressure.

In particular, at the stagnation point (where the center line of the exhaust flow meets the surface) the stagnation pressure, $P_s$, is written

$$P_s = \frac{k+2}{2} P_r \left(\frac{h}{r_n}\right)^{-2} \qquad (2\text{-}3)$$

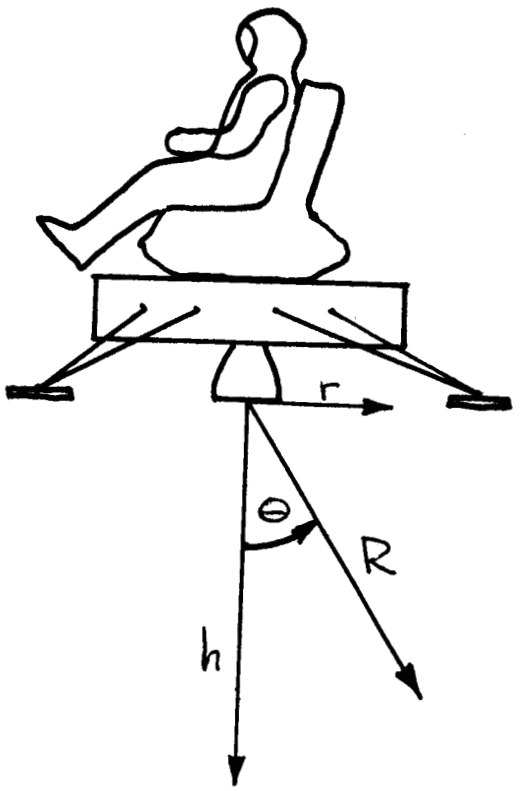


FIGURE 2-2. JET EXHAUST COORDINATE SYSTEM

The temperature, T, of the fluid near the surface at any radial distance may be established using

$$\frac{T}{T_s} = \left(\frac{P}{P_s}\right)^{\frac{\gamma-1}{\gamma}} \tag{2-4}$$

where $T_s$ is the stagnation temperature which does not change across the shock. Also, because there is no heat transfer across the shock the steady-flow energy equation may be written

$$U^2 + 2c_p T = \text{constant} \tag{2-5}$$

where

$U$ = velocity of the gas

$c_p$ = specific heat at constant pressure

therefore,

$$U^2 = 2c_p(T_s - T) \tag{2-6}$$

Substituting Eqs. (2-2) through (2-4) into Eq. (2-6) yields for $U_c$

$$U_c^2 = 2c_p T_s \left[1 - (\cos\theta_c)^{\frac{(k+4)(\gamma-1)}{\gamma}}\right]$$

or

$$U_c^2 = 2c_p T_s \left\{1 - \frac{h^2}{h^2+r_c^2}^{\frac{\left[\gamma(\gamma-1) M_n^2 + 4\right](\gamma-1)}{2\gamma}}\right\} \tag{2-7}$$

where $\theta_c$ = the value of $\theta$ corresponding to $r_c$.

The density of the fluid at any radial position downstream of the shock, based on the assumption of a perfect gas, can be calculated

from the relation

$$\rho = \frac{P}{R_o T} \quad \text{(downstream of shock)} \tag{2-8}$$

where

$R_o$ = Specific gas constant.

## 2.3 Dust/Debris Entrainment

### 2.3.1 Velocity of Entrained Particles

Each particle, once it breaks free of the lunar surface, is subjected to a drag force by the rocket exhaust. Based on a preliminary theoretical study combined with an analysis of motion pictures from reference 7, the most significant time period, during which the particle accelerates to some maximum velocity, $V_d$, occurs prior to the particle leaving the edge of the crater as shown in Figure 2-3. Thus, it is convenient to express the maximum velocity as

$$V_d = C_e \rho_c^{\frac{1}{2}} U_c \tag{2-9}$$

where

$C_e$ = entrainment coefficient

$\rho_c$ = gas density at crater edge

$U_c$ = gas velocity at crater edge.

The entrainment coefficient is a dimensional parameter which is directly proportional to the drag coefficient and cross-sectional area of the particle, and the time interval, $t_e$, during which the drag force

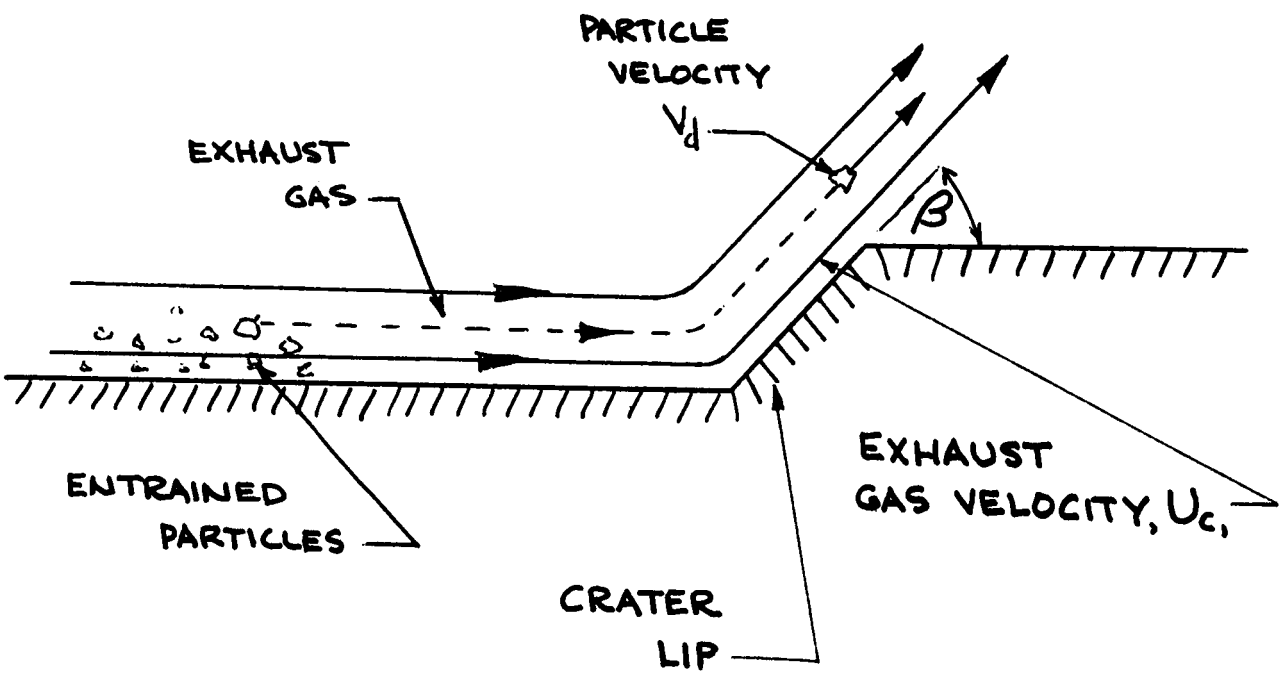


FIGURE 2-3. ENTRAINMENT OF DUST AND DEBRIS

accelerates the particle, and inversely proportional to the mass of the particle. The velocity, $U_c$, is considered to be the most characteristic velocity associated with the exhaust impingement. Generally speaking, the particle velocity, $V_d$, will occur as the particle leaves the tip of the crater. Thus, the assumption is made that

$$V_d \leq U_c \tag{2-10}$$

The maximum value of $C_e$ is then considered to be

$$C_{e\ max} = \rho_c^{-\frac{1}{2}} \tag{2-11}$$

It is important to note that the velocities achieved by individual particles in the experimental investigation, described in reference 6 and shown in reference 7, were sufficiently large to cause several of the illumination lamps used in that experiment to be smashed by impact of the flying debris.

### 2.3.2 Path of Entrained Particles

The assumption is made that the drag force acting on the particle, following deflection at the crater lip, is small compared to that drag force occurring prior to deflection. This assumption is based on the fact that the density of the exhaust gases should decrease rapidly following deflection at the crater lip. With this assumption, in the immediate vicinity of the impingement crater, the behavior of the particles can be satisfactorily described in a two-dimensional rectangular coordinate (x, y) system. The velocity components are thus

$$V_x = V_d \cos(\beta) \tag{2-12}$$

$$V_y = V_d \sin(\beta)\, g_m t \tag{2-13}$$

where

$V_x$ = velocity in the x direction

$V_y$ = velocity in the y direction

$g_m$ = acceleration due to lunar gravity

$t$ = time,

and the space coordinates are

$$x = V_d \cos(\beta)t \tag{2-14}$$

$$y = V_d \sin(\beta)t - \frac{g_m t^2}{2} \tag{2-15}$$

The above equations neglect the spherical shape of the moon which is reasonable for short distances. However, due to the low lunar gravity and the possibility of high particle velocities, the distance or range which such particles may travel may be large. Thus, for calculating range, it is necessary to use a more accurate dynamic analysis, involving particle behavior in a central force field. For this case, the range, S, is

$$S = R_m \left[ 2 \arccos \left( \frac{p - R_m}{eR_m} \right) \right] \tag{2-16}$$

where

$$p = \frac{R_m^2 V_d^2 \cos^2(\beta)}{\mu_m} \tag{2-17}$$

$$e = \left[1 + \frac{R_m V_d^2 \cos^2(\beta)}{\mu_m} \left(\frac{R_m V_d^2}{\mu_m} - 2\right)\right]^{\frac{1}{2}} \qquad (2\text{-}18)$$

with

$\mu_m$ = lunar gravitational constant ($.0173 \cdot 10^{16}$ ft$^3$/sec$^2$)

$R_m$ = lunar radius ($.570 \cdot 10^7$ ft).

Notice should be taken that when

$$e = 1$$

or

$$\frac{R_m V_d^2}{\mu_m} = 2$$

an escape trajectory is achieved.

### 2.3.3 Maximum Radius of Impingement Crater

The primary force tending initially to set a particle in motion is a surface shearing force, $F_s$, which can be expressed as

$$F_s = \tau_s A_{ef} \qquad (2\text{-}19)$$

where

$\tau_s$ = shear stress

$A_{ef}$ = effective particle area.

The initial resistance to motion is the static friction force of the particles, $F_f$, which may be written

$$F_f = f_d \rho_d v_d g_m \qquad (2\text{-}20)$$

where

$f_d$ = static friction factor of dust ( = tan $\beta$)

$\rho_d$ = density of dust particles

$v_d$ = volume of a individual particle

$g_m$ = lunar gravitational acceleration.

Erosion of a particular portion of a dust-covered surface is considered to occur when $F_s > F_f$. The friction force, $F_f$, is a function solely of the lunar surface characteristics. If these are relatively constant within a given region, the impingement erosion pattern will be symmetrical and will extend out to some maximum radius $r_c$ beyond which $F_s \leq F_f$. This radius is thus the maximum crater radius for a particular jet exhaust at a fixed height above the surface. For specific values of f, $\rho_d$, $v_d$, and $A_{ef}$ a crater radius can be established if the shear stress, $\tau_s$, can be calculated. Based on a combination of the theories presented in references 4 and 5, this shear stress can be espressed as

$$\tau_s = (1.312)\, r\, \rho \left(\frac{\mu}{\rho_s}\right)^{\frac{1}{2}} \left(\frac{4\rho\, c_p\, T}{\rho_r h^2}\right)^{3/4} \qquad (2\text{-}21)$$

where

$\rho$ = density of gas

$\rho_s$ = stagnation density of gas

$\rho_r$ = normal shock recovery density of gas

$= \rho_o \left(1 + \gamma M^2\right) \left(1 + \frac{\gamma - 1}{2} M_n^2\right)^{-\frac{1}{\gamma - 1}}$

$\rho_o$ = chamber density of gas

$\gamma$ = ratio of specific heat ($C_p/C_v$)

$M_n$ = Mach number at nozzle exit

$\mu$ = viscosity of gas

$c_p$ = specific heat at constant pressure

$T$ = temperature of gas

$r$ = radial position.

Examination of Eq. (2-21) reveals that the predicted $\tau_s$, as to be expected, is a function of the radial position and the physical properties of the exhaust gas. While $\tau_s$ would appear to increase with r, it decreases with decreasing gas density, temperature, and viscosity, which are all functions of radial position. Careful analysis of the rate of decrease of these three properties with increasing radius indicates that for large values of r, $\tau_s$ approaches zero. The relationship between $F_s$ and $F_f$ for a typical impingement crater is shown in Figure 2-4.

As indicated by Figure 2-4, in the vicinity of the stagnation point, the shear force is less than the static friction force. As a result of this inequality, the crater is initially annular in shape (refs. 1, 3, 5, and 8). Gradually, as the impingement process continues, the central portion of the annulus is eroded away, leaving the more familiar bowl-shaped crater.

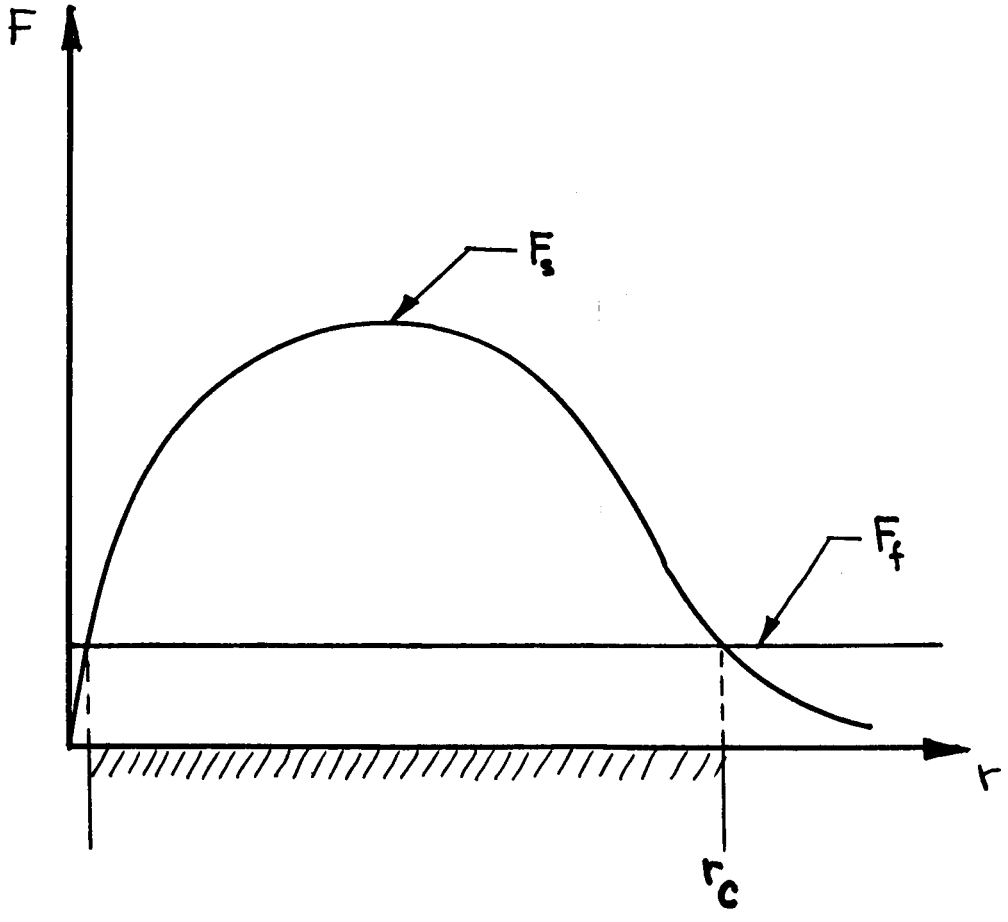


FIGURE 2-4. RELATIONSHIP BETWEEN $F_s$ AND $F_f$ FOR A TYPICAL IMPINGEMENT CRATER

## 3.0 DISCUSSION OF RESULTS

Based on a careful examination of the impingement phenomenon, there appear to be three types of hazards which might occur as a result of dust or debris being set in motion by the exhaust gases of the MFS. These hazards are: (1) decreased visbility during ascent or descent of the MFS due to the cloud of dust/debris, (2) dust or debris striking some portion of the MFS, and (3) dust or debris striking equipment or personnel on the lunar surface in the vicinity of the point of impingement.

The first hazard listed was investigated in reference 6. The results of reference 6 clearly indicate that some decrease in visibility will occur, but this will be temporary and will not be as severe as would occur in the presence of an atmosphere such as that of Earth. Because of time and manpower limitations, coupled with the complexity of the problem, no attempt was made in the present study to predict the degree of reduced visibility. Instead, major attention was directed toward calculating the nature of the second and third hazards.

### 3.1 Possibility of Dust/Debris Striking the MFS

By means of the equations developed in Section 2.0, the path of particles in the vicinity of the MFS during ascent or descent was calculated. In carrying out these calculations it was necessary to select appropriate values of various parameters characteristic of the MFS. These parameters and the values selected are presented in Table 3-1. The angle $\beta$ was held at 50° because this represents the maximum

TABLE 3-1

Selected Values of MFS Parameters

| Parameters | Value |
|---|---|
| Diameter of nozzle ($d_e$) | 5.81 in |
| Expansion ratio ($\varepsilon$) | 40 |
| Mach number at exit ($M_n$) | 5.5 |
| Ration of specific heats ($\gamma$) | 1.26 |
| Thrust (F) | 100 lb |
| Mixture ratio (M.R.) | 1.6 |
| Specific Impulse ($I_{sp}$) | 295 sec |
| Chamber pressure ($P_c$) | 85 psia |
| Chamber temperature ($T_c$) | 5542 °R |
| Maximum diameter of MFS | 9.0 ft |
| Number of rocket engines | 5 |

value for this angle which is considered to be appropriate for the lunar dust. Figures 3-1 and 3-2 represent the paths of particles for various crater radii and heights, respectively. In both figures, in order to ensure that the upper limit to such paths were established, the value of the entrainment coefficient was set equal to the reciprocal of the square root of the gas density at the crater lip. As indicated by these figures the possibility of dust/debris striking the MFS is greatest at low altitudes with small crater radii.

The critical height at which there is a strong probability of dust/debris striking the MFS is presented in Figure 3-3. Again $\beta$ has been set equal to 50°. As indicated in Table 3-1, the maximum diameter of the MFS was taken to be nine feet. As before, the entrainment coefficient was set equal to the reciprocal of the square root of the gas density at the crater lip. These critical heights only occur when the crater radius is less than 4.5 feet. At such small heights as are involved, the crater radius will quite likely exceed this limiting value, especially during descent. For thick layers of dust, or during ascent from an undisturbed surface, however, impingement on the MFS appears likely to occur.

A careful study of Figures 3-1, 3-2, and 3-3 indicates that there is also the possibility that the particles will strike vertical lunar surfaces, such as large crater walls. A ricocheting effect could then occur which might result in dust/debris striking the MFS from above or from the side.

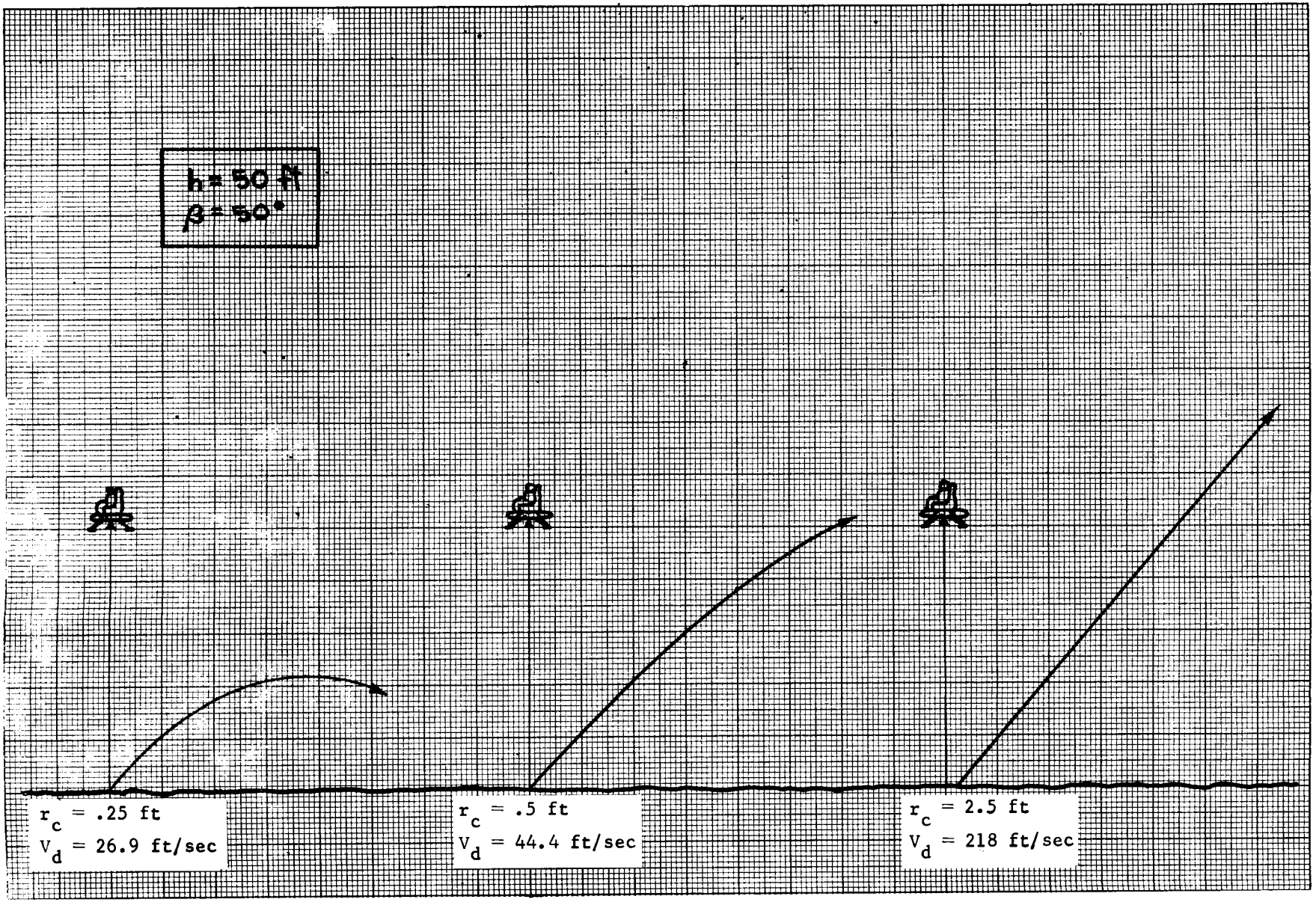


FIGURE 3-1. EFFECT OF IMPINGEMENT CRATER RADIUS ON DUST PARTICLE PATH

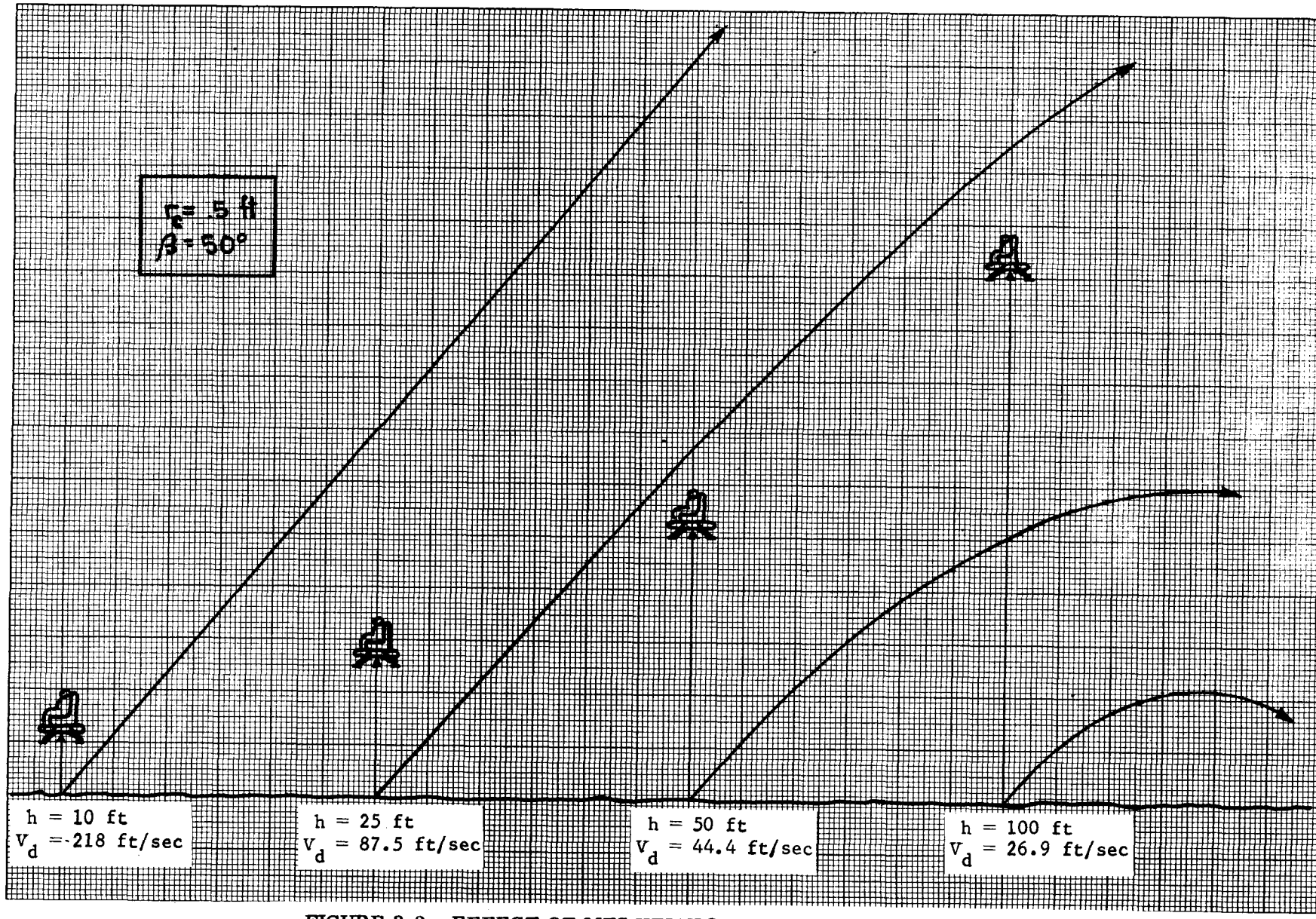


FIGURE 3-2. EFFECT OF MFS HEIGHT ON DUST PARTICLE PATH

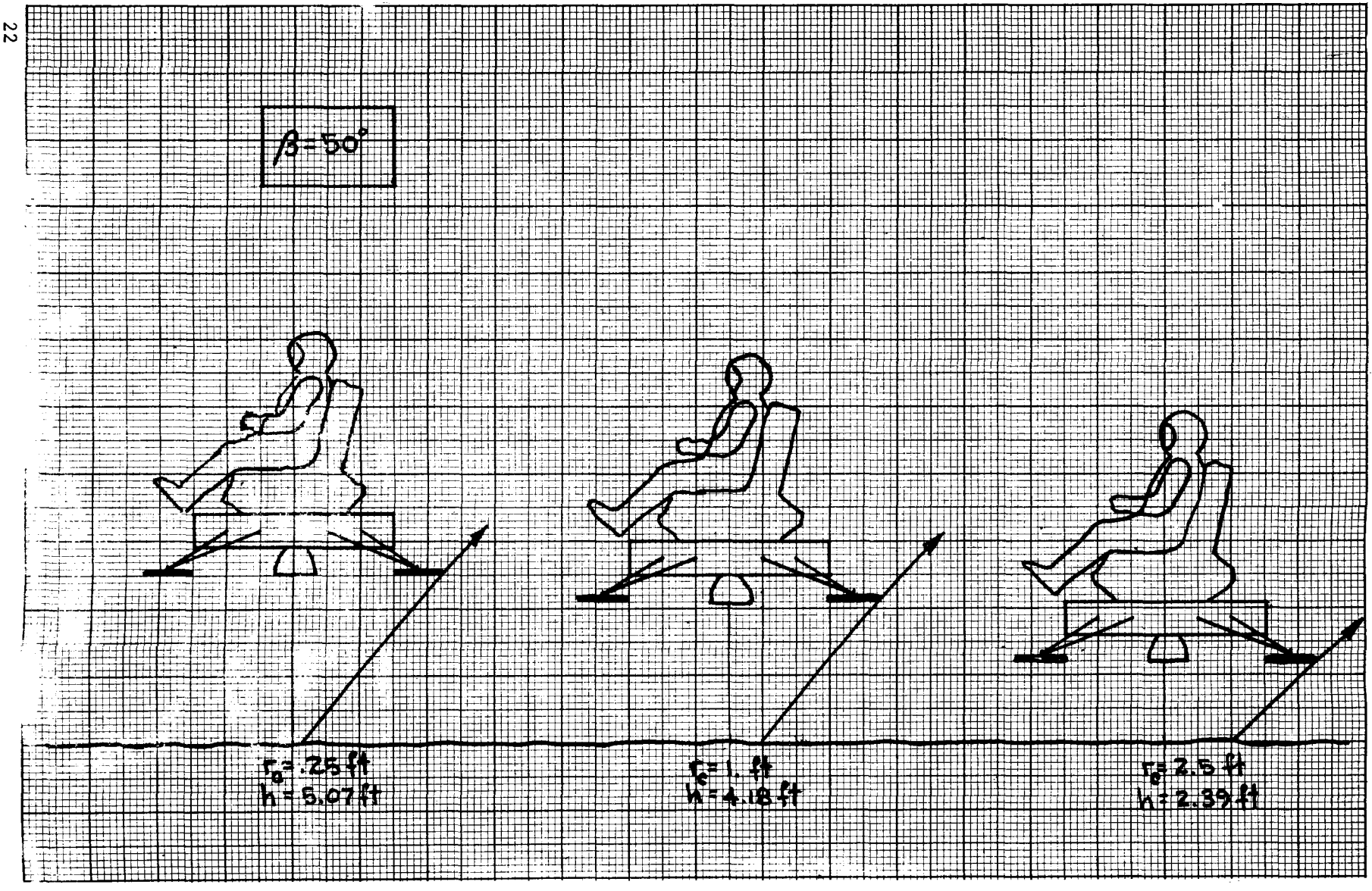


FIGURE 3-3. CRITICAL HEIGHTS FOR VARIOUS CRATER RADII

## 3.2 Dust/Debris Danger Zone

The velocities, $V_d$, which the dust/debris could achieve were found to range as high as several thousand feet per second. By means of Eq. (2-16) the ranges associated with such velocities were calculated for various values of $\beta$ and $\theta_c$ and various entrainment coefficients. The maximum range, out to which particles may be projected, are presented in Table 3-2 for $\theta_c$ equal to 30°, 45°, and 60° with entrainment coefficients equal to 10%, 50%, and 100% of the reciprocal of the square root of the exhaust gas density. In this table, that value of $\beta$ was used which produced the maximum range.

As indicated by Table 3-2, the danger zone extends out to a considerable distance. In this regard, heavier particles would be characterized by the smaller entrainment coefficients while lighter particles would tend to have the maximum value of $C_e$.

TABLE 3-2

Dust/Debris Danger Zones

| $\theta_c$ (deg) | $C_e$ $(\frac{ft^{3/2}}{lb_m^{\frac{1}{2}}})$ | $V_d$ $(\frac{ft}{sec})$ | S(miles) |
|---|---|---|---|
| 30 | $.1\ (\rho_c)^{-\frac{1}{2}}$ | 229 | 2.27 |
| | $.5\ (\rho_c)^{-\frac{1}{2}}$ | 1144 | 47.4 |
| | $1.0\ (\rho_c)^{-\frac{1}{2}}$ | 2290 | 208.0 |
| 45 | $.1\ (\rho_c)^{-\frac{1}{2}}$ | 350 | 5.31 |
| | $.5\ (\rho_c)^{-\frac{1}{2}}$ | 1750 | 116.0 |
| | $1.0\ (\rho_c)^{-\frac{1}{2}}$ | 3500 | 568.0 |
| 60 | $.1\ (\rho_c)^{-\frac{1}{2}}$ | 484 | 9.1 |
| | $.5\ (\rho_c)^{-\frac{1}{2}}$ | 2420 | 236 |
| | $1.0\ (\rho_c)^{-\frac{1}{2}}$ | 4840 | 1230 |

## 4.0 CONCLUSIONS

Based on the material presented in the preceding section the conclusion is reached that the dust/debris set in motion by the impingement on the lunar surface of the exhaust gases of the Manned Flying System does represent several hazards. This conclusion is based, of course, on the assumption that the lunar surface is covered with dust and/or debris to some degree. The hazards involved include reduced visibility, striking of the MFS by flying dust/debris, and striking of personnel and equipment on the lunar surface in the general vicinity of the impingement site.

Because of the simplified engineering model employed in this study, the results obtained should not be considered to be anything more than a preliminary estimate of the nature of the impingement and entrainment phenomena. Before truly accurate prediction of these phenomena can be made, a more advanced theoretical model must be developed and tested by comparison with all existing experimental data.

## 5.0 REFERENCES CITED


1. Stitt, Leonard, E., "Interaction of Highly Underexpanded Jets with Simulated Lunar Surfaces", NASA-TN-D-1095, Lewis Research Center, December 1961.

2. Bauer, R. C. and R. T. Schlumpf, "Experimental Investigation of Free Jet Impingement on a Flat Plate", AEDC-TN-60-223, Arnold Engineering Development Center, March 1961.

3. Spady, A. A., Jr., "An Exploratory Investigation of Jet-Blast Effects on a Dust-Covered Surface at Low Ambient Pressure", NASA TN-D-1017, Langley Research Center, February 1962.

4. Roberts, Leonard, "The Action of a Hypersonic Jet on a Dust Layer", IAS Paper No. 63-50, IAS 31st Annual Meeting, January 1963.

5. Sibulkin, M. and W. H. Gallaher, "Some Aspects of the Interaction of a Jet with a Dust Covered Surface in a Vacuum Environment", ERR-AN-244, General Dynamics/Astronautics, 10 February 1963.

6. Hurt, G. J., Jr. and L. J. Linn, "Blast Effects of Twin Variable-Cant Rocket Nozzles on Visibility During Landing on a Particle-Covered Surface", NASA TN-D-2455, Langley Research Center, December 1964.

7. Hurt, G. J., Jr. and L. J. Linn, Film Supplement L-689 to NASA TN-D-2455, Langley Research Center, December 1964.

8. Land, N. S. and L. V. Clark, "Experimental Investigation of Jet Impingement on Surfaces of Fine Particles in a Vacuum Environment", NASA TN D-2633, Langley Research Center, February 1965.

9. Stark, R. L., "An Analysis of Skewed Supersonic Rocket Nozzles", Masters Thesis, University of Alabama, June 1965.

## DISTRIBUTION

INTERNAL

DIR
DEP-T
R-DIR
R-AERO-DIR
-S
-SP (23)
R-ASTR-DIR
-A (13)
R-P&VE-DIR
-A
-AB (15)
-AL (5)
R-RP-DIR
-J (5)
R-FP-DIR
R-FP (2)
R-QUAL-DIR
-J (3)
R-COMP-DIR
-RSP
R-ME-DIR
-X
R-TEST-DIR
-I
I-DIR
MS-IP
MS-IL (8)

EXTERNAL

NASA Headquarters
MTF Col. T. Evans
MTF Maj. E. Andrews (2)
MTF Capt. Bart Cambell
MTF Mr. D. Beattie
R-1 Dr. James B. Edson
MTF William Taylor

Kennedy Space Center
K-DF Mr. von Tiesenhausen

EXTERNAL

Northrop Space Laboratories
Huntsville Department
Space Systems Section (5)

Scientific and Technical Information Facility
P. O. Box 5700
Bethesda, Maryland
Attn: NASA Representative (S-AK/RKT) (2)

Manned Spacecraft Center
Houston, Texas
Mr. Gillespi, MTG
Mr. Dornbach ET-33
C. Corington, ET-23 (1)
William E. Stoney, ET (2)

Donald Elston
Manned Lunar Exploration Investigation
Astrogeological Branch
USGS
Flagstaff, Arizona

Langley Research Center
Hampton, Virginia
Mr. R. S. Osborn